Synthesis of Cu-Al-Ni Shape-Memory Alloy Using Simple Metallurgical Practices

Matthew Beaudouin-Lafon, Leon Lam, Sam Myers, Katerina Soltan

***Abstract*—Shape-memory alloys (SMAs) are able to return to their original shape when heated to a relatively low temperature after deformation [1]. Nickel titanium (Ni-Ti) produces the most robust alloy for shape-memory purposes and has a variety of uses in the engineering and medical fields. However, the titanium component makes it very expensive and difficult to manufacture. Copper-based SMAs (Cu-Al-Ni in particular) are used as alternatives to Ni-Ti alloys as they are easier and cheaper to produce. Despite their potential benefits, copper-based SMAs are more brittle, possess lower shape recover strains than Ni-Ti, and are very sensitive to composition.**

In this study, we attempt to synthesize a Cu-Al-Ni SMA using simple metallurgical processes. While phases with twinned structures characteristic of SMAs are present in our final sample, the expected phase transformations from martensite to austenite are absent.

I. INTRODUCTION

SMAs are a class of materials "able to remember a predetermined configuration and to recover it as consequence of thermal or mechanical loads" [2]. They exhibit a shape-memory effect, the ability of a material to be deformed at a low temperature and then revert to its prior shape upon heating [3].

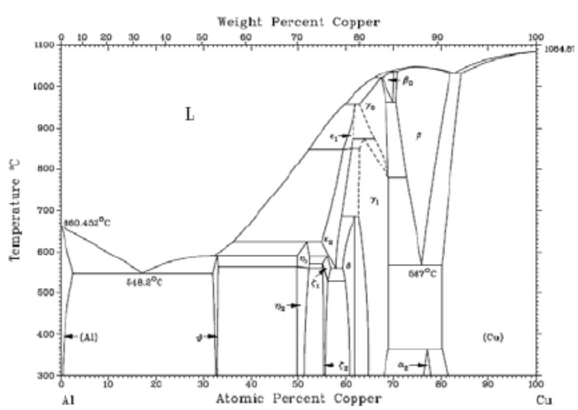

Fig. 1: While the alloy studied included a tertiary component, nickel, the binary phase diagram of the Cu-Al system was used for analysis [4]. The addition of nickel expands the β phase across a wider range of aluminum contents, and slows down the diffusion of copper and aluminum atoms to form the γ_1 + α phase [5].

The shape-memory effect of Cu-Al-Ni alloys comprises of three stages, and depends on the reversibility of the austenite (β) $\rightarrow$ self-accommodating martensite (β') phase transition. To "set" the shape-memory, the metal is heated to $900°C$, turning everything into the β phase. When quenched rapidly, the Cu-Al eutectoid decomposition $\beta \rightarrow \alpha + \gamma_1$ at $567°C$ is prevented (see Fig. 1 for a phase diagram); instead, a $\beta \rightarrow \beta'$ transition occurs [5]. The addition of nickel slows the diffusion of copper and aluminum, allowing the alloy to reach the temperature of the martensitic transformation before changing phase.

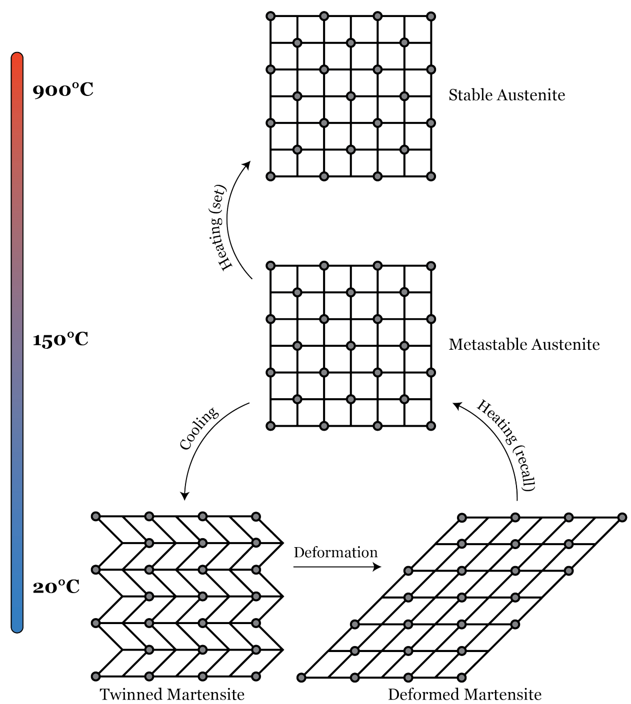

Fig. 2: Shape-memory dynamics: The martensite can deform without breaking any bonds. When heated, it returns to the austenite phase with the original shape, again without breaking any bonds.

The β' martensite forms in a twinned configuration, with many variants of the same structure occurring in different crystallographic orientations which relieve the overall stress and strain of a system, resulting in no visible change in shape [6]. Upon deformation, the variants orient themselves in the same direction, as shown in Fig. 2, resulting in a detwinned martensite which can easily shift back into the metastable austenite parent phase without breaking any bonds [7], [8].

To "recall" the shape, the metal is heated to $150°C$ where β' transforms into the metastable parent phase, β. While β is not the lowest energy, stable phase at $150°C$, the transformation from β' to β is diffusionless and only requires a distortion of the lattice, whereas transformation to γ_1 + α requires diffusion and therefore more energy [7]. The transformation happens very rapidly, quickly bringing the metal to the set shape, as the crystals return to a body centered cubic structure [5]. If held at this temperature, the austenite phase will undergo a diffusion transformation to the stable γ_1 + α phase.

SMAs are used in a variety of applications: their shape-memory effect, relatively light weight, and high elasticity allow them to be used as actuators and springs in fields ranging from jet engine design for their high energy density, to small-scale tremor cancelling devices for their high work density, and orthodontics to exert constant tooth-moving forces on the teeth [9], [10], [11].

Our goal was to make an alloy from base components that displays shape-memory effects using simple manufacturing techniques, and to learn about the dynamics behind shape-memory alloys.

II. Experimental Procedure

According to existing literature, the optimal composition of Cu-Al-Ni alloys for shape-memory effect is 4 wt.$\%$ nickel and between 11 and 14 wt.$\%$ aluminum by weight [5], [12], [8]. While most synthesis procedures involve advanced techniques such as melt extraction, we used simple casting and heat treatment techniques in an attempt to synthesize a shape-memory alloy [13].

The raw materials - 86.4 g of pure copper wire, 13.5 g of compressed aluminum powder, and 4.2 g of pure nickel - were melted in a graphite crucible in an induction furnace with approximately 3 grams of boric acid. The intended composition was 83 wt.$\%$ Cu, 13 wt.$\%$ Al, and 4 wt.$\%$ Ni.

The alloy underwent two 60 s heating, 60 s isothermal, 30 s cooling cycles in an (60-60-30), and three 30-30-10 cycles, and was stirred in the cooling phase of each cycle except for the last. During the last cooling cycle, the molten alloy was poured onto a copper plate angled at about 40 degrees above a bucket of room-temperature water. The intent was to allow the alloy to spread out on the highly thermally conductive copper plate and begin cooling rapidly into a thinner sheet of material, which would then fall into the water to be fully quenched. The melting and quenching was then repeated a second time to ensure that all materials were uniformly mixed.

Half of the quenched alloy was annealed for 30 minutes at $900°C$ and quenched to ensure martensitic transformation, so as to homogenize the sample in the austenite phase before cooling [14]. Samples of both heat-treated and as-cast alloys were then analyzed. Samples embedded in phenolic powder were ground with SiC papers, polished to 0.05 micron alumina, and etched using 2 parts H_2SO_4, 1 part 3$\%$ H_2O_2, and 2 parts H_2O to study their microstructure with a scanning electron microscope (SEM) and optical microscopy. Compositional analysis was also performed with the SEM. Shavings of the samples were used in differential scanning calorimetry (DSC) tests at $10°C$/min to check for the reversible martensite - austenite phase transition which gives SMAs their shape-memory effect.

III. Results and Discussion

Compositional Analysis

The energy disperive x-ray spectrometer (EDS) was used to determined an 11 wt.$\%$ aluminum and 4 wt.$\%$ nickel composition in the resulting samples. It is important to note that the aluminum composition is lower than the expected 13 wt.$\%$. A possible cause of this phenomenon is that the alloy did not fully mix when casted, despite remelting our sample twice. While the resulting pieces were visually uniform by eye on the inside (if looking at a cross section), the outside of the sample had distinct yellow and silver colored parts, suggesting higher copper and aluminum content, respectively. Traces of boron were detected in the darker regions of the cast, suggesting some form of reaction with the boric acid in the crucible during melting. Darker spots also had a higher aluminum composition, suggesting the precipitation of the γ_1 phase, as shown in Fig. 3.

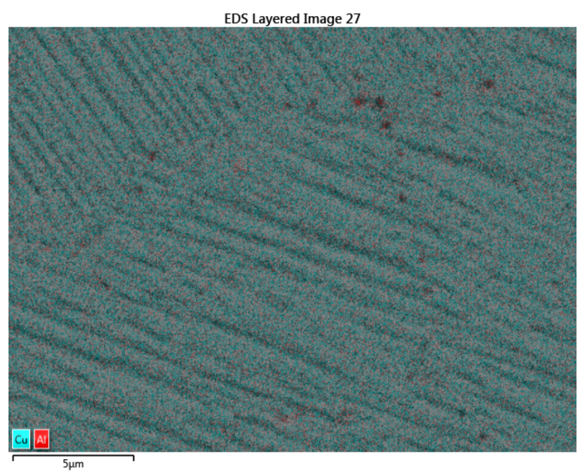

Fig. 3: SEM micrograph with EDS compositional map overlay. The red spots correspond to the higher aluminum concentration nucleating phase (γ_1).

Microstructure Analysis

The microstructure of the non-annealed sample (Fig. 4) exhibited small silver and brown grains surrounded by larger areas of the same color, suggesting that the sample was not quenched rapidly enough to prevent precipitation of another phase. Precipitation of copper-rich α and aluminum-rich γ_1 could have caused diffusion of their major components throughout the metal, resulting in larger surrounding areas with the same color. SEM composition analysis supports this observation, as larger percentages of aluminum were detected in close proximity to the small, darker grains. These are less apparent in the annealed sample (Fig. 5).

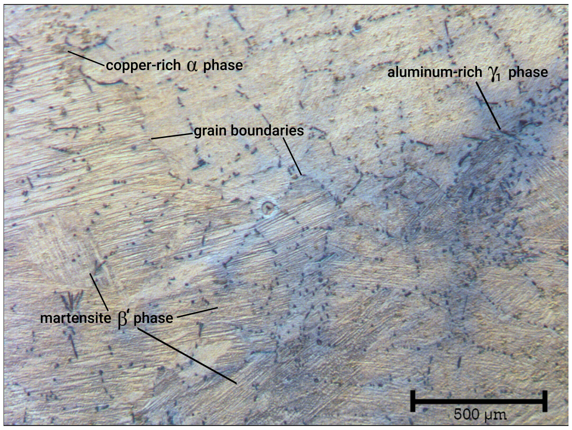

Fig. 4: Optical micrograph of non-heat-treated sample. Etchant: 2 parts H_2SO_4 : 1 part 3% H_2O_2 : 2 parts H_2O. The non-heat treated sample exhibited copper-rich α and aluminum-rich γ_1 precipitant phases, seen as the orange and silver, respectively, colored sections along the dark grain boundaries. Striped sections, with a variety of orientation, are most likely the martensitic β' phase. However, the prevalence of α and γ_1 suggests that the sample was not quenched rapidly enough to facilitate a uniform $\beta \rightarrow \beta'$ transformation.

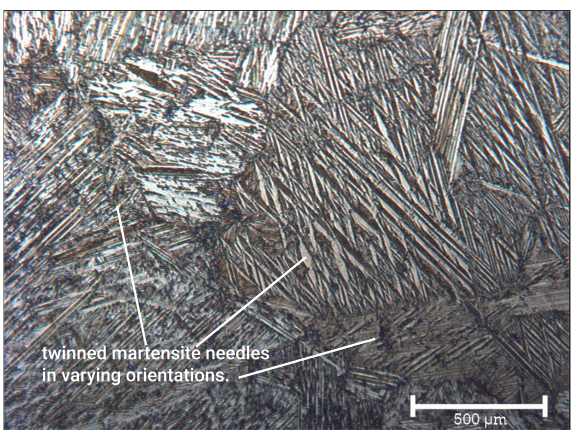

Fig. 5: Optical micrograph of annealed sample. Etchant: 2 parts H_2SO_4 : 1 part 3% H_2O_2 : 2 parts H_2O. The annealed sample's clearly twinned needle shaped microstructure oriented in various directions is characteristic of the martensite β' phase, seen as parallel strips of light and dark material. The heat treatment increased both the size and uniformity of the needles, reducing the growth of α and γ_1 precipitants seen in the non-annealed sample.

The characteristic striped and needle-like pattern of the β' martensite is present in both samples, although it is more uniform in the heat-treated one. The different directions of the stripes represent the twinned martensite variants, as they are structurally the same but have different crystallographic orientations. The needles themselves tend to be larger in the annealed sample, most likely because annealing decreases the number of nucleation sites, allowing the martensite to grow uninhibited.

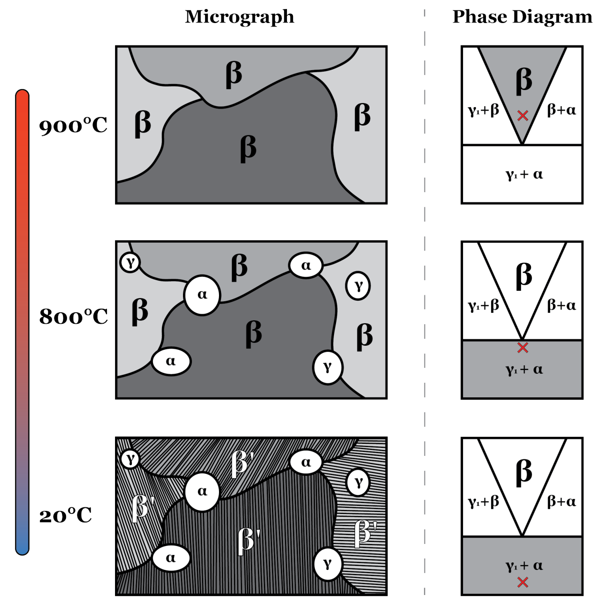

Fig. 6: SMA microstructure formation: As the β phase cools, the α and γ_1 phases nucleate, until all of the β transforms into the martensitic β'.

Grains of the non-heat treated sample were on the order of 3 mm^2 while the annealed sample had grains around 2 mm^2, their large sizes indicating a non-ductile material. While larger grains are usually more ductile, the casting process introduces an accumulation of defects at the grain boundaries, resulting in a tendency to form cracks in the brittle area between grains when stressed rather than propagating dislocations through the large grains that can deform to accommodate them. While the samples were not tested for hardness or ductility, they were qualitatively very brittle and hard, which is consistent with literature stating that Cu-Al-Ni SMAs may be less favorable due to their brittleness [5], [1], [15]. Heat treatments are recommended to improve the ductility of copper-based alloys, allowing molecules to diffuse into positions relieving stress and recrystallizing into a more uniform lattice. However, the new grain growth is not guaranteed to retain its original structure (i.e., martensite) and requires a heat treatment to be highly controlled; the use of grain refiners like manganese or boron has been found to be more successful [1], [16]. Due to the alloy's high sensitivity to heat treatment, it is not unlikely that we were not able to control the annealing process well enough to effectively improve its mechanical properties.

Shape-Memory Effect

While optical analysis of our samples suggests the possibility that an alloy with shape-memory properties was formed, DSC results (Fig. 7) contradict this hypothesis. Shape-memory effect appears on a DSC curve as a phase transformation exhibiting hysteresis: the starting temperature of the austenite to martensite transformation is different than that of the reverse transformation, martensite to austenite [6].

For copper-aluminum-nickel SMAs, this transformation happens between $50°C$ and $200°C$ [1], [12]. SMAs are very sensitive to thermal cycling, which can introduce dislocations or destroy the shape-memory effect by changing the occurring transformation (to γ_1 + α for example) [17]. It is possible that the DSC cycles that were run eliminated most of the martensite phase, or that other precipitating phases are preventing the martensite transformation.

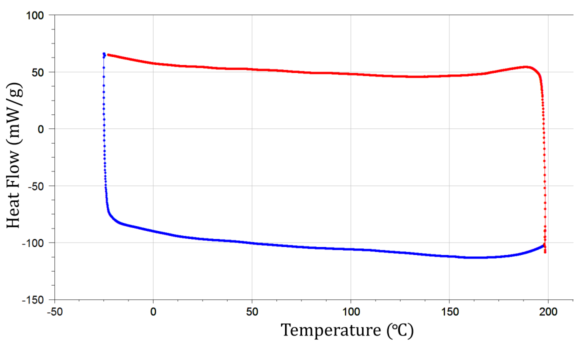

Fig. 7: Differential scanning calorimetry profile of the annealed sample. No significant phase transformations suggesting shape-memory effect are present.

IV. Conclusion

While Cu-Al-Ni shape-memory alloys are easier to manufacture than Ni-Ti, they are not suited to simple casting techniques where composition and temperature are not easily controlled. Although the microstructure typical of SMAs was present in the produced samples, we found no evidence of shape-memory effects.

Acknowledgment

We would like to thank Professor Matt Neal and Professor Jon Stolk for all of the help and support throughout this project. The authors would also like to thank the empty dining hall milk dispenser and the *soft* cookies.

References

[1] V Sampath. Studies on the effect of grain refinement and thermal processing on shape memory characteristics of cu–al–ni alloys. *Smart materials and structures*, 14(5):S253, 2005.

[2] Thomas W Duerig, KN Melton, and D Stöckel. *Engineering aspects of shape memory alloys*. Butterworth-Heinemann, 2013.

[3] Kenneth E Wilkes and Peter K Liaw. The fatigue behavior of shape-memory alloys. *JOM*, 52(10):45–51, 2000.

[4] Yanhong Tian, Chunjin Hang, Chunqing Wang, and Y Zhou. Evolution of cu/al intermetallic compounds in the copper bump bonds during aging process. In *Electronic Packaging Technology, 2007. ICEPT 2007. 8th International Conference on*, pages 1–5. IEEE, 2007.

[5] AC Kneissl, E Unterweger, M Bruncko, K Mehrabi, G Lojen, and H Scherngell. Microstructure and properties of niti and cualni shape memory alloys. *Metalurgija*, 14(2):89–100, 2008.

[6] Darel E Hodgson, WH Ming, and Robert J Biermann. Shape memory alloys. *ASM International, Metals Handbook, Tenth Edition.*, 2:897–902, 1990.

[7] Osman Adiguzel. Self-accommodating nature of martensite formation in shape memory alloys. *Solid State Phenomena*, 213:114, 2014.

[8] Kenneth Kanayo Alaneme and Eloho Anita Okotete. Reconciling viability and cost-effective shape memory alloy options – a review of copper and iron based shape memory metallic systems. *Engineering Science and Technology, an International Journal*, 19(3):1582 – 1592, 2016.

[9] Frederick Calkins, G Butler, and James Mabe. Variable geometry chevrons for jet noise reduction. In *12th AIAA/CEAS Aeroacoustics Conference (27th AIAA Aeroacoustics Conference)*, page 2546, 2006.

[10] Anupam Pathak. *The development of an antagonistic SMA actuation technology for the active cancellation of human tremor*. PhD thesis, University of Michigan, 2010.

[11] Fujio Miura, Masakuni Mogi, Yoshiaki Ohura, and Hitoshi Hamanaka. The super-elastic property of the japanese niti alloy wire for use in orthodontics. *American Journal of Orthodontics and Dentofacial Orthopedics*, 90(1):1–10, 1986.

[12] V Recarte, RB Pérez-Sáez, J San Juan, EH Bocanegra, and ML Nó. Influence of al and ni concentration on the martensitic transformation in cu-al-ni shape-memory alloys. *Metallurgical and Materials Transactions A*, 33(8):2581–2591, 2002.

[13] Dong-yue Li, Shu-ling Zhang, Wei-bing Liao, Gui-hong Geng, and Yong Zhang. Superelasticity of cu–ni–al shape-memory fibers prepared by melt extraction technique. *International Journal of Minerals, Metallurgy, and Materials*, 23(8):928–933, 2016.

[14] S.H. Chang. Influence of chemical composition on the damping characteristics of cu–al–ni shape memory alloys. *Materials Chemistry and Physics*, 125(3):358 – 363, 2011.

[15] Gorazd Lojen, Ivan Anžel, A Kneissl, A Križman, E Unterweger, B Kosec, and M Bizjak. Microstructure of rapidly solidified cu–al–ni shape memory alloy ribbons. *Journal of Materials Processing Technology*, 162:220–229, 2005.

[16] J. Gui, W.H. Zou, R. Wang, D. Zhang, C.H. Tang, M.Z. Xiang, and D.Z. Yang. X-ray diffraction study of the reverse martensitic transformation in cu-al-ni-mn-ti shape memory alloy. *Scripta Materialia*, 35(3):435 – 440, 1996.

[17] MO Lai, L Lu, and WH Lee. Influence of heat treatment on properties of copper-based shape-memory alloy. *Journal of materials science*, 31(6):1537–1543, 1996.